Proceedings of the 2024 Winter Simulation Conference
H. Lam, E. Azar, D. Batur, S. Gao, W. Xie, S. R. Hunter, and M. D. Rossetti, eds.

SURROGATE MODEL FOR DISTRIBUTION NETWORKS INFLUENCED BY WEATHER

Juan M. Restrepo, James Nutaro, Chris Sticht*, Teja Kuruganti

Oak Ridge National Laboratory, Oak Ridge, TN, USA
* Idaho National Laboratory, Idaho Falls, ID, USA

ABSTRACT

We propose a method for generating reduced representations of time series and for constructing low dimensional surrogate models for time dependent calculations of power and voltage in distribution networks. We employ Fourier polynomials. The surrogate model strategy is aimed at reducing the computational cost of time dependent simulations, albeit, at the expense of fidelity. The reduced representation is achieved by identifying a small and most consequential subset of degrees of freedom. In power and voltage distribution networks dynamics that are heavily influenced by strong cyclic weather events, *e.g.*, the hourly, diurnal and seasonal cycles, the weather/climate time series spectrum exposes these most energetic components. Once the degrees of freedom are identified their amplitudes are optimized using training data. The key challenge in using spectral methods in power network surrogates is addressing the computation of quotients. For this we propose a numerically-stable deconvolution strategy.

1 INTRODUCTION

Data-driven approaches to surrogate modeling can preserve a significant amount of fidelity when compared to a fully resolved model counterpart. See (Jiang, Zhou, and Shao). However, these methods are often ad-hoc and yield surrogate models that function as black boxes. Further, the training often involves a significant amount of data and computation. We propose a trigonometric interpolation strategy to create a reduced representation of distributed network data and a surrogate model based on the same, aimed at reducing the computational cost of distributed network and circuit models, for problems that are strongly influenced by cyclic phenomena, such as those present in climate and weather dynamics. An attractive feature of Fourier interpolation is a natural connection of the network's dynamics to the cyclic variations in climate, weather, and demand for power.

Cyclic behaviors in distributed networks are sufficiently pronounced that they play an integral role in load forecasting (Almeshaiei and Soltan 2011; Al-Alawi and Islam 1996). See also (Hu et al. 2019), (Rastogi et al. 2021) and the context of control (Olama et al. 2020). Moreover, these cyclic variations are growing in significance as renewable generation becomes an increasingly important source of electricity. For weather-influenced power performance the Fourier method makes it easy to infer correlations between weather cyclicity (e.g., diurnal and seasonal variations) and that of the network, yielding intepretability in a surrogate generated by trigonometric interpolation.

Our proposed method trades fidelity for computational efficiencies by eliminating frequency components that make small contributions to the solution. However, it is not solely based upon a low or band pass filtering. The surrogate could be useful in generating quick network condition estimates critical to rapid robust decisions, for example, in renewable power networks, however, the use of Fourier methods comes with numerical challenges. In this paper we address these and suggest numerically efficient and stable ways to overcome them.

To be clear, not every distributed network output or performance displays significant sensitivity to weather and climactic conditions; ideally these conditions are to be avoided. However, and especially with the greater reliance on renewable sources that happen to be weather sensitive, it is more common to see

whole or parts of a distribution network performance to be influenced by weather, and perhaps climate. For power signals or for distributed network models that have a strong weather/climate signature, the proposed data and model surrogate could be a useful computational tool. In what follows it will be understood that we are focusing on weather-sensitive signals and distribution networks.

2 SURROGATE MODEL IN THE FREQUENCY DOMAIN

For any time dependent variable, $F(t)$ say, over time spans of a few years we expect a cyclic component associated with weather and seasonal variation and a linear trend that becomes increasingly pronounced over sufficiently long time scales. The latter encodes a linearized drift due to climate variations. Our model is intended to capture the cyclic behaviors that dominate system dynamics, not ignoring climate drift. Therefore, we decompose the signal $F(t)$, with equally-spaced samples at time $t_n \in [t_0, t_S]$, into a linearized trend $\alpha + \beta t_n$ and a cyclic remainder. Thus

$$F(t_n) = \alpha + \beta t_n + f(t_n) \ , \ n = 0, 1, \ldots, S$$

where α and β are constants estimated by least-squares. The linear trend $\alpha + \beta t$ corresponds to climate drift.

For $f(t_n)$, after standard periodization strategies are applied, so that f is now t_S-periodic (the periodization of $f(t)$ removes artifices and improves the spectral accuracy of the trigonometric interpolation), we assume a complex trigonometric polynomial representation of the form

$$\begin{aligned} f(t_n) &= \sum_{j=-S/2+1}^{S/2} \hat{f}(\omega_j) e^{i\omega_j t_n} \ , \ n = 0, 1, \ldots, S-1 \\ \hat{f}(\omega_j) &= \frac{1}{S} \sum_{n=0}^{S} f(t_n) e^{-i\omega_j t_n} \ , \ j = -\frac{S}{2} + 1, \ldots, S \end{aligned} \tag{1}$$

where $\hat{f}$ are the complex coefficients. In what follows let $\mathscr{F}(\omega)$ denote the discrete Fourier transform of $f(t)$ and its inverse by $\mathscr{F}^{-1}$.

The reduced model will be a trigonometric approximation $\tilde{f}(t)$ of $f(t)$, with s degrees of freedom, where $s \ll S$, defined for $t_0, t_1, ..., t_S$. One reduction strategy is to use some criteria for picking frequencies ω, possibly among the ω_j, and amplitudes $\hat{f}(\omega)$, possibly $\hat{f}(\omega_j)$. The strategy we follow here is to pick among the ω_j trigonometric basis, informed by the weather, and use some criteria to find their corresponding (complex) amplitude $\hat{f}$, not necessarily $\hat{f}(\omega_j)$. We will develop the latter strategy. The motivation for this strategy is illustrated by the top of Figure 1a. The figure shows power demand fluctuations, denoted as $\delta P(t)$, at a specific location in a distribution network (the signal is synthetic but inspired by actual local electric utility meter reports; the signal has been stripped of its mean value and modified in amplitude). The hours mark time relative to January 1 at 12am, 2022. The readings were taken every hour, over the course of one year, for a total of 8,760 entries. Figure 1b shows the time series after it is reshaped lexicographically, with hours per day and days per year as axes. The reshaping makes explicit the diurnal cyclicity, and to a lesser extent, seasonality, of the signal.

The corresponding approximation to $f(t_n)$ retains significant elements from the two distinct time scales while discarding the rest. The resulting form of the model is

$$\tilde{f}(t_n) := \sum_{j \in J_L} \hat{f}(\omega_j) e^{i\omega_j t_n} + \sum_{j \in J_H} \hat{f}(\omega_j) e^{i\omega_j t_n}, \tag{2}$$

for $t_n = 0$, t_1, ..., t_S where J_L are the low frequency components, associated with seasonal variations, and J_H are the high frequency components associated with daily variations. The main question is which elements to retain while maintaining an acceptable bound on the approximation error.

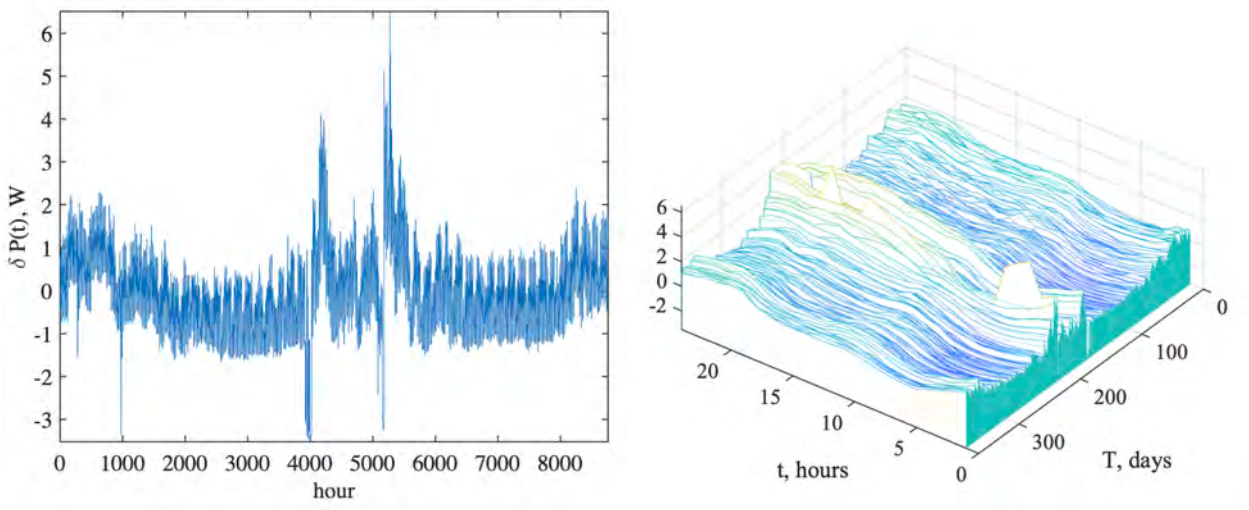

(a) (b)

Figure 1: (a) Detrended power signal $\delta P(t)$; (b) the same time series, lexicographically organized, or reshaped, in 24 hour increments. The signal is based upon an historical record of power usage in a residential unit, taken over one year at 1 hour intervals.

Given sets J_L and J_H the approximation error is

$$\max_{0\le t_n\le t_S} |f(t_n)-\tilde{f}(t_n)|^2 \le \sum_{\omega_j\in S\setminus J} |\hat{f}(\omega_j)|^2, \tag{3}$$

where $J = J_L \cup J_H$. This is the familiar global error for spectral interpolation, which presumes that the amplitude $\hat{f}$ in $\tilde{f}$ for the terms included are identical to the $\hat{f}$ of f itself. However, if the $\hat{f}$ in $\tilde{f}$ are allowed to be something else, one has to resort to an empirical error. The total energy in the signal and the estimate in (3) provide guidance, but are not sharp bounds on the error, and hence, one needs to work with an empirical threshold.

A alternative expression for the error involves transforming the reduced signal back into the time domain. In this case, using our selected s components and $\hat{f}$ in $\tilde{f}$ seek to satisfy

$$|f(t_n)-\tilde{f}(t_n)|^2 \le \text{TOL} \tag{4}$$

where TOL is a non-negative empirical error threshold, and the condition is satisfied at s of the t_n locations. The fact that TOL is not a priori generally determined suggests two approaches to determining a sparse representation of the signal in terms of a fixed set of frequencies.

Method 1 (sparse) emphasizes sparsity (low $s < S$), accepting larger TOL values to accommodate energy shortfalls in the approximation. Here, we work with the reshaped data. Without loss of generality we will assume that the data was collected hourly over 1 year.

To find the frequencies associated with J_L we perform the discrete/fast Fourier transform (FFT) along the day axis, producing 24 FFTs. For each of these we normalize the modulus of the Fourier coefficient to the largest one in each hour. We identify, on each hour, the frequencies with the largest normalized moduli and we make use of (3) to establish an amplitude cutoff. The set of frequencies in J_L is the union of the most energetic among all 24 FFTs.

To establish the set of frequencies in J_H we have 365 FFTs in the hour axis, perform a similar search. Next, we use (4) to fix the amplitudes at these given frequencies. A Monte Carlo process would then be performed in which each sample chooses a different set of s of t_n locations, and the problem will be one of determining the coefficients such that (4) in the expectation is satisfied.

Method 2 (energy) emphasize energetic consistency, accepting possibly a larger s than in Method 1. The set J_H is found as in Method 1. However, in choosing the set in J_L we pick all frequencies below some threshold.

Let ω_L belong to a frequency in the daily range. Hence,

$$\tilde{f}(t_n) := \sum_{j=-L}^{L} \hat{f}(\omega_j) e^{i\omega_j t_n} + \sum_{j \in J_H} \hat{f}(\omega_j) e^{i\omega_j t_n}, \tag{5}$$

where $L < S$ and L not in J_H. Basically, we are thresholding in the frequencies associated with daily motions, and we are retaining only frequencies that have importance in the hourly data. The amplitudes of the components in J_H are picked as in Method 1, and the amplitudes associated with $\omega_j \leq \omega_L$ are set by fulfilling (3).

3 USING THE SURROGATE REPRESENTATION

The computational challenge posed by adopting trigonometric polynomials to build a practical surrogate for power/voltage networks is that products of signals in the time domain become convolutions in the frequency domain. Hence, convolutions/de-convolution operations need to be addressed in a numerically stable manner.

To illustrate the challenge and a possible practical solution, consider the power flow calculations for a distributed network with N current loops or bus components. The power at time t_n at the k^{th} element is found by solving

$$P_k(t_n) = V_k(t_n) \sum_{j=1}^{N} Y_{kj}(t_n) V_j(t_n) e^{i\phi_{kj}}, \quad t_n = t_0, t_1, ..., t_S, \tag{6}$$

where P is power, V is the voltage, Y is the admittance or the inverse of the impedance Z, and ϕ the phase. We note here that we allow for the admittance to be time dependent. Solving this problem in the time domain for S time steps requires S solutions of the power flow equations.

In the frequency domains, only a single solution is required but that solution involves a convolution of the s components in our surrogate model. Specifically, if we write (6), for each t_n, as

$$P_k(t_n) = V_k(t_n) M_k(t_n), \quad k = 1, 2, ..., N \tag{7}$$

where $M_k(t_n) = \sum_{j=1}^{N} Y_{kj}(t_n) V_j(t_n) e^{i\phi_{kj}}$ then, in Fourier space, the equations to be solved are

$$P(\omega_\ell) = \frac{1}{2\pi} V(\omega_\ell) \star M(\omega_\ell), \tag{8}$$

where $\star$ conveys the convolution operation, $P(\omega) = \mathscr{F} P(t)$, for $\ell = 0, 1, .., S-1$, and $k = 1, 2, .., N$. For the time dependent case, there is a non-linear solve which is often done at each time step by some bisection, fixed point or higher order iteration scheme, presuming conditions are right for a unique fixed points to exist at each time step. In the Fourier case, and presuming the same conditions on fixed points, the iteration is done over all of frequencies at once.

To compute the convolution in a numerically stable manner we rewrite, for $\ell = 0, 1, .., S-1$, (8) as

$$P(\omega_\ell) = \frac{1}{2\pi} H_V^S M(\omega_\ell),$$

where H_V^S is an anti-cyclic matrix of dimension S. If we instead use s interpolants, and H_V^s we obtain a reduced representation of the variables. The explicit form of H_V^S will be made plain in a calculation that follows. (Success in this calculation requires that the variables be periodic, which might require pre-processing data for periodization via extensions).

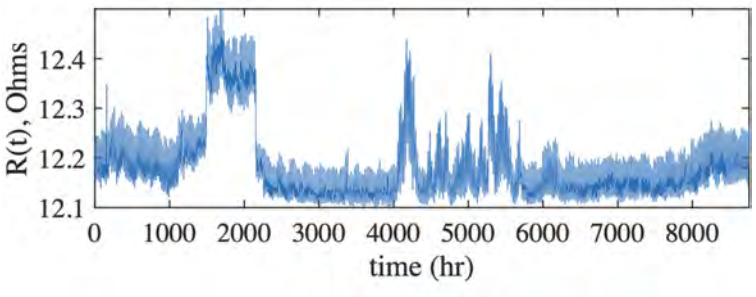

Figure 2: Time series for $R(t)$, used in the surrogate model example calculation.

3.1 A Sample Calculation

We restrict our example to a simple circuit calculation to emphasize the construction and use of the convolution matrix H_V. A generalization to power flow calculations is straightforward, but the necessary iterative procedure reduces the illustrative power of the more complete problem.

Consider a circuit with $N = 1$ loop currents $I(t)$, voltage sources $E(t)$, power $P(t)$, and $N \times N$ (real) impedance matrix $R(t)$. The goal of this calculation is to develop a surrogate and use it to calculate the unknown voltage and power and compare these to the time dependent non-reduced values, we denote as the 'exact' solution. The simple system is given:

$$R(t_n)I(t_n) = E(t_n)\ ,\ t_n = t_0, ..., t_S \quad \text{and} \tag{9}$$

$$E(t_n)I(t_n) = P(t_n). \tag{10}$$

We use the power data shown in Figure 1a for $\delta P(t)$. Another time synthetic time series is used for $R(t)$ and is inspired by another local utility record. $R(t)$ is shown in Figure 2. We will solve for the unknowns $I(t)$ and $E(t)$. The time dependent benchmark is solved in a straightforward manner using (9)-(10). For the estimate, on the other hand, we employ Method 1 and 2 to find surrogates of $R(t)$ and $P(t)$, and we use (9)-(10) to solve for the surrogates of $I(t)$ and $E(t)$ using the same s Fourier components we used to capture R and P in Fourier space and then transform back to real time.

If we cast

$$P(t) = p_0 + \delta P(t) = p_0 + p_1 t + p(t) \text{ and}$$
$$R(t) = r_0 + \delta R(t) = r_0 + r_1 t + r(t)$$

the terms $p_0 + p_1 t$ and $r_0 + r_1 t$ are the 'climate' linear trends, and $r(t)$ and $p(t)$ are the 'weather' cyclic terms. Apparently in 2022, when this data was collected, the trend was downward: $p_0 = 3.6545$ W, $p_1 t = -3.281 \times 10^{-5} t$ W, and $r_0 = 12.223\,\Omega$, $r_1 t = -8.455 \times 10^{-6} t\,\Omega$, respectively.

The spectrum of $\delta P(t)$ is shown in Figure 3. To begin, we reshape δP and δR (see Figure 1). We then analyze the 24 yearly $T-$time series $\delta P(T)$ and $\delta R(T)$, and the 365 daily $t-$time series $\delta p(t)$ and $\delta r(t)$. The spectra of each of the T and, respectively, the t series, were similar enough that we simply produced an ensemble average T-time series and a $t-$ time series.

3.1.1 Method 1 (sparse)

We analyze the averaged T-time series for δP and δR. Figure 4.

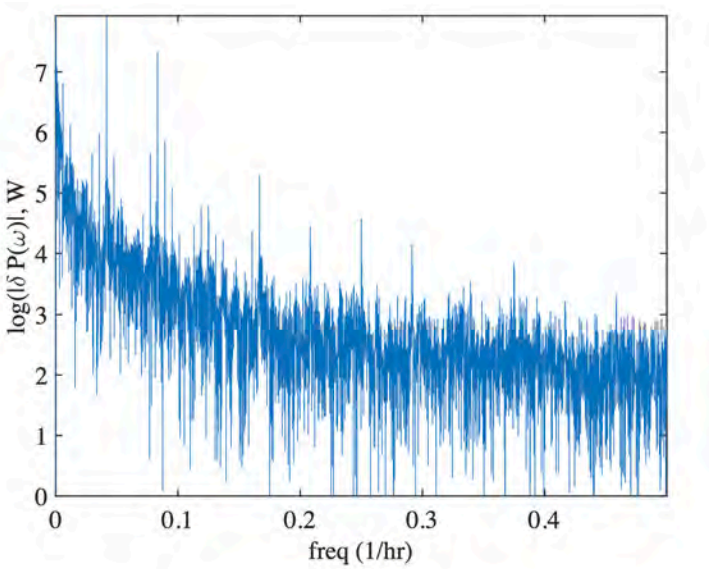

Figure 3: Spectrum of $\delta P(t)$. $\delta P(t)$ appears in Figure 1 in its original and its reshaped form.

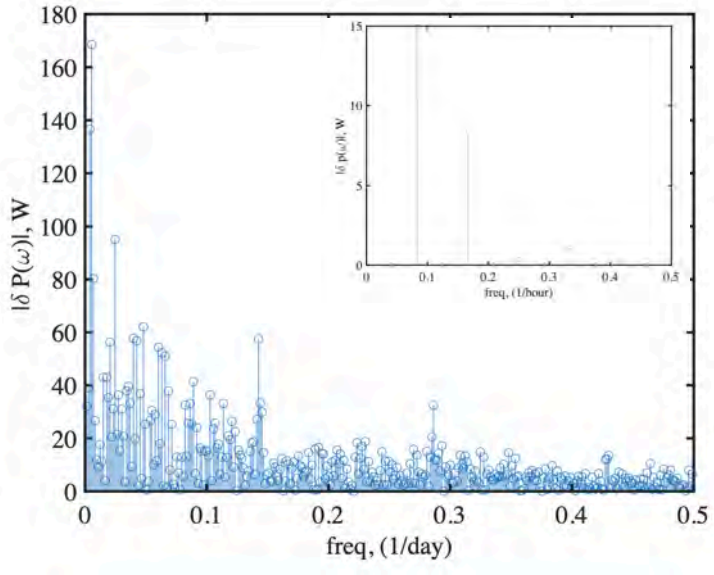

Figure 4: Modulus of the Fourier coefficients of the discrete Fourier transform of the ensemble averaged $T-$time series $\delta P(T)$. Inset, Fourier modulus for $t-$series $\delta p(t)$, respectively.

We construct trigonometric approximations of the form

$$\tilde{\delta}P(T) = \sum_{|l|\in J_L\setminus 0} \hat{\delta}P(\Omega_l)e^{i\Omega_l T},$$
$$\tilde{\delta}R(T) = \sum_{|l|\in J_L\setminus 0} \hat{\delta}R(\Omega_l)e^{i\Omega_l T}$$

where Ω_l are the frequencies on the day time scale, and T is in units of days.

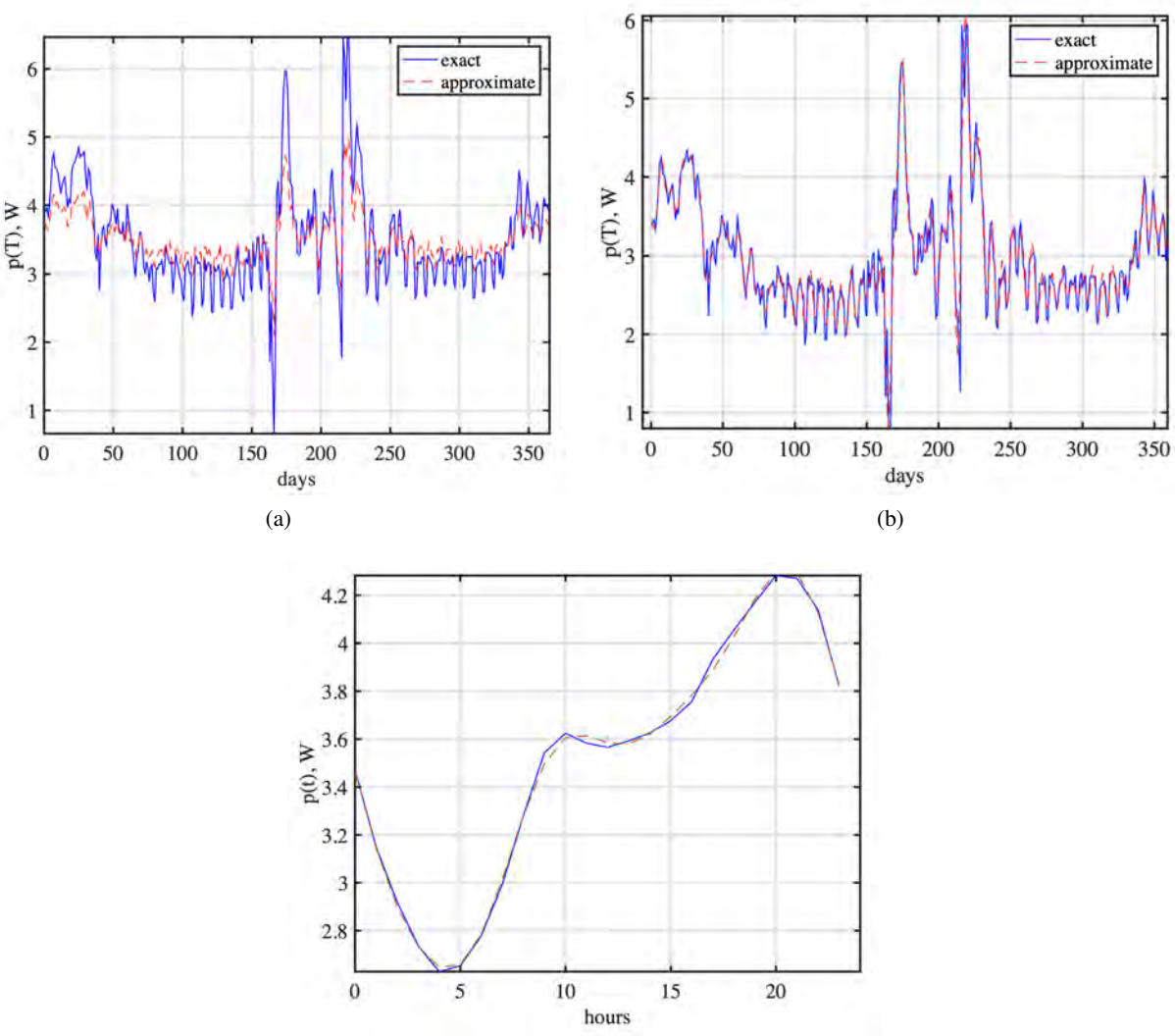

Figure 5: Comparison of the exact (solid) and the approximate time series (dashed). (a) $\delta P(T)$ (a) Method 1 and (b) Method 2; (c) $\delta p(t)$, for both methods.

In this method we rank-order the amplitude of spectral components (normalizing these to the highest component), and based upon their modulus amplitude we add them to the set J_L. We then tune the amplitudes using an empirical threshold $0 \leq \text{TOL} \leq 1$. We perform a similar process on the t-time series, creating an approximation of the form

$$\tilde{\delta} p(t) := \sum_{|l| \in J_H \setminus 0} \hat{\delta} p(\omega_l) e^{i\omega_l t}, \quad \tilde{\delta} r(t) := \sum_{|l| \in J_H \setminus 0} \hat{\delta} r(\omega_l) e^{i\omega_l t}$$

where ω_l are frequencies in the hour scale and t is in units of hours.

The parameter TOL was set to 0.1, sifting 61 daily modes (J_L) and 4 hourly modes (J_H), for a total of $s = 65$ modes. The amplitudes of the reconstruction were then optimized according to (4). In Figure 5a we show a comparison of the exact $T-$daily signal for P using Method 1.

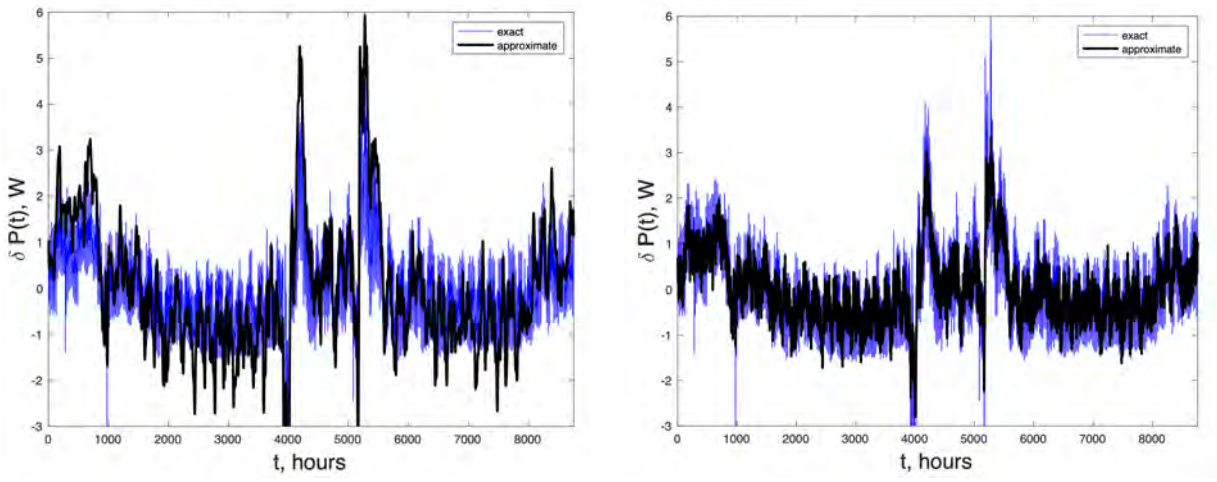

(a) (b)

Figure 6: Method 1. Comparison of the exact (solid) and the approximate time series (dashed) on $\delta P(t)$. (a) using only the J_L modes (b) adding the J_H modes.

3.1.2 Method 2 (energy)

Method 2 picks the individual hourly frequencies, and we threshold the frequencies associated with daily frequencies. Using the same value for TOL, we obtain the comparison shown in Figure 5b. The results are qualitatively better than in Method 1, albeit we used 126 (J_L) Fourier interpolants for the $T-$time series and 4 (J_H) for the $t-$time series. In this case we are using a total of $s = 130$ modes. The final step for either method is to assemble the approximation of the S-long time series. We will only show δP. For each respective method, we assemble (2).

In Figure 5 there are marked differences in the reconstruction of the dayly time series, between both methods. The tolerance was the same in both methods; a tighter fit would be obtained with Method 1 using a smaller tolerance (Figure 5a). In Figure 6 we show a comparison of $\delta P(t)$ and its approximation using Method 1. In Figure 6a we show the approximation using only the J_L modes and amplitudes. In Figure 6b we add the J_H modes. In contrast, Figure 7 shows a comparison of $\delta P(t)$ and its approximation using Method 2. Figure 7a displays the comparison of the exact and its approximation using only the J_L modes and amplitudes. In Figure 7b we add the J_H modes.

3.1.3 Surrogate Model

In this paper we define a surrogate model as a set of reduced Fourier representation of coupled equations. The structure of the equations is inherited from the primitive time dependent equations the Fourier equations derive from. The coefficients of the individual trigonometric interpolants are derived by Method 1 or 2, to approximately satisfy the primitive equations. The surrogate model, built using Method 2, will be used to calculate $I(t)$ and $E(t)$. This requires solving for the coefficients of the Fourier polynomial approximation for $I(t)$ and $E(t)$, the s Fourier modes will be the 130 modes that were used to determine the approximation for $P(t)$ and $R(t)$. To solve for the coefficients of the 2 unknowns we work in Fourier space using (9) and (10). For each $\ell \in J_L \cup J_H$,

$$\begin{aligned}
\frac{1}{2\pi} Z(\omega_k - \omega_\ell) I(\omega_\ell) &= E(\omega_\ell)\ ,\ k \in J_L \cup J_H \\
\frac{1}{2\pi} I(\omega_k - \omega_\ell) E(\omega_\ell) &= P(\omega_\ell)\ ,\ k \in J_L \cup J_H.
\end{aligned} \tag{11}$$

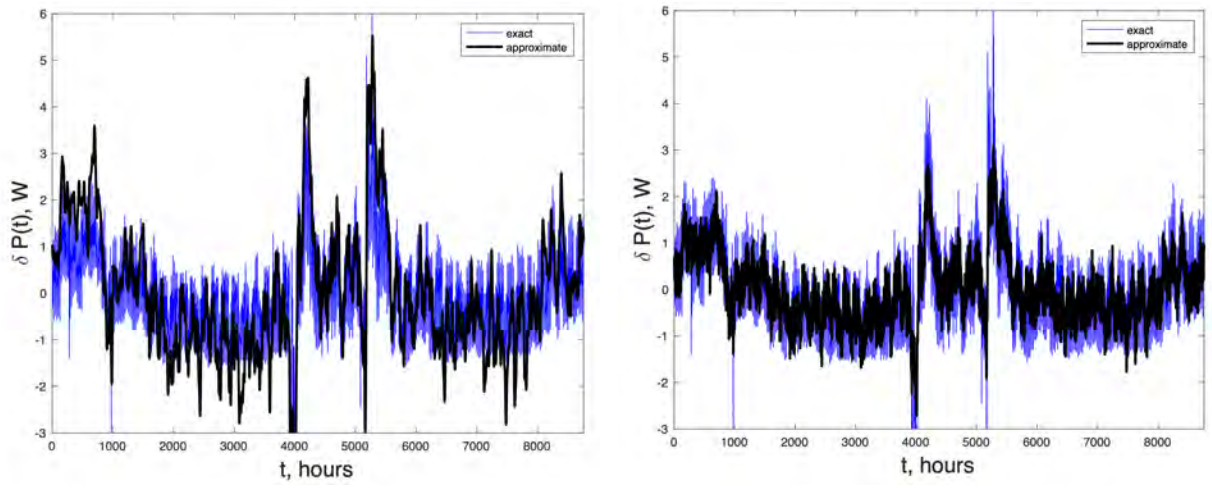

(a) (b)

Figure 7: Method 2. Comparison of the exact (solid) and the approximate time series (dashed) on $\delta P(t)$. (a) using only the J_L modes (b) adding the J_H modes.

To solve for $I(\omega)$ and by a fixed point method for $E(\omega)$ we will need to perform deconvolutions.

Conventional deconvolution is generally numerically unstable. Hence, crucial to making the use of a Fourier-based surrogate that is practical, we need to propose an alternative procedure. The key to solving the system is to convert the convolution into the matrix problem

$$H_Z^s I(\omega_\ell) = E(\omega_\ell), \tag{12}$$

H_Z^s is a matrix of size $s \times N$ per side, for N loops, corresponding to N currents. The exact solution is obtained when $s = S$.

For $N = 1$ the exact calculation (that is, with $s = S$), the H_Z^S convolution matrix

$$\begin{bmatrix} Z(0) & -Z(S-1) & -Z(S-2) & \cdots & -Z(2) & -Z(1) \\ Z(1) & Z(0) & -Z(S-1) & \cdots & & \vdots \\ \vdots & \vdots & \vdots & \cdots & & \vdots \\ & & & \cdots & Z(0) & -Z(S-1) \\ Z(S-1) & Z(S-2) & \cdots & \cdots & Z(1) & Z(0) \end{bmatrix}$$

is an $S \times S$ matrix, the argument of each entry is the frequency index. The matrix H_Z^s is of size $s \times s$, if the reduced representation is used. The computational complexity of the convolution is $\mathscr{O}(S^2)$, which when compared to the $\mathscr{O}(S)$ of the conventional time dependent methodology, hardly justifies its use. However, if we use surrogates and these are of dimension $s < S$, it is possible that the dimensions of the surrogate are such that $s^2 < S$, in which case the convolution methodology gains practical currency.

Figure 8 shows the results of using the deconvolution and Method 2 to solve for the current and the electromotive potential, as a function of time. We choose here to display the comparison of the exact and the surrogate approximation in Figure 8 the T-time daily evolution of the current and potential and in the inset, the corresponding counterparts for $t-$time.

4 COMPUTATIONAL COMPLEXITY

For an S element time series, the computational complexity of the reduced Fourier representation is $s < S$. Additionally, there are 2 fast Fourier transforms (FFT), along with some additional processing.

For the surrogate model, the computational complexity is application specific. We will merely highlight the cost estimates for key operations that arise in calculations such as the ones encountered in power networks,

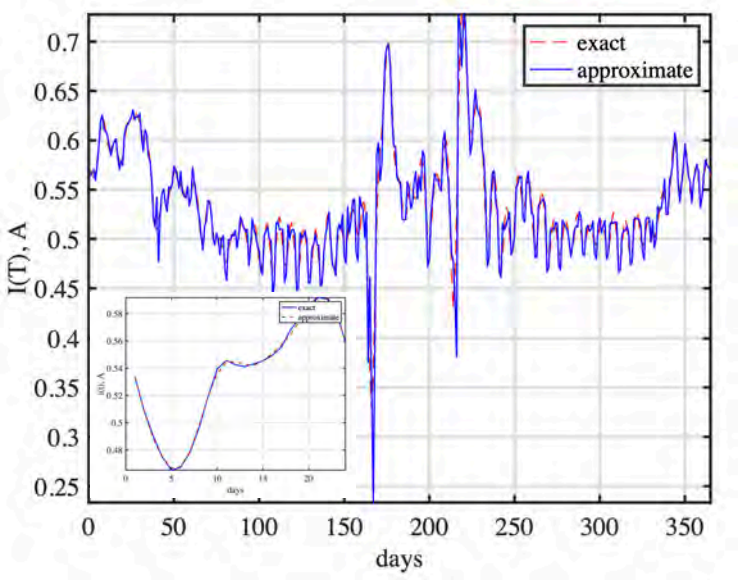

Figure 8: Method 2: Superposition of the surrogate approximation and the exact solution; The current $I(T)$. Inset: comparison of reduced (dots) and exact $I(T)$ year-long current.

i.e., typified by Equation (6) or for distribution circuits, *i.e.*, Equations typified by (9)-(10). The cost of vector multiplication in time as compared to vector convolution; the cost of deconvolution; the cost of matrix-vector multiply and its Fourier counterpart; the cost of simple fixed point iteration.

The multiplication of two scalar time series of size S require s^2 operations in Fourier, hence, as long as $s^2 < S$, there is a saving in required operations (ignoring FFT costs). In both the power and the loop current calculations there are matrices of size N, where N is the number of loops. A matrix-vector multiply, over S time steps would thus require N^2S operations. The (reduced) convolution involves s frequencies, so the cost is N^2s^2. In the loop calculations the inversion of the impedance matrix is required, S times. Supposing we use QR, for example, the cost is N^3S in the time domain. In the frequency domain, inverting and convolving would cost N^3s^2. In summary, the reduced representation model is computationally-competitive when $s^2 < S$.

For $N = 1$ one can deconvolve by inverting $H_Z^s = QR$, where Q is unitary and R is an upper triangular matrix. This is the process used in the computational examples shown above. For example, (12) becomes, for $\ell = 0, 1, ..., S-1$,

$$\hat{C}(\omega_\ell) := Q\hat{E}(\omega_\ell) \quad \text{and} \quad \hat{I}(\omega_\ell) = R\hat{C}(\omega_\ell) \ . \tag{13}$$

Once $\hat{I}(\omega_\ell)$ is obtained, using (13), $I(t)$ is obtained by taking an inverse Fourier transform. The QR decomposition cost is $\mathscr{O}(S^3)$. (A sparse algorithm is used in practice and thus the above inversion cost is usually pessimistic). Clearly, the reduced Fourier case, in which H_Z^S is replaced by H_Z^s is especially effective in reducing the computational cost of the QR inversion. Parenthetically, the smaller s is, the better conditioned will be the convolutional matrix, presuming that there are significantly fewer modes in J_H than in J_L.

Regarding the solution of (9) and (10), a fixed point iteration is involved to solve for all of the variables, and in the time dependent case, the fixed point iteration is usually performed at each time step, at a cost of $\mathscr{O}(S \times J_t)$, where J_t is the typical number of interations per time step. In Fourier, the fixed point iteration is done for each frequency, at a cost $\mathscr{O}(s \times J_\omega)$ (alternatively, over all Fourier coefficients simultaneously). Hence, the approximate Fourier will be more efficient if $J_t \approx J_\omega$, and $s < S$.

5 CONCLUSIONS

The goal of this project was to develop a computationally efficient polynomial approximation of observational data as well as a general procedure to generate surrogate models of time dependent distributed network models. In approximating time series, the strategy achieves a significant data representation reduction, albeit at the expense of fidelity. In creating surrogate models of time dependent processes, its practical goal is reducing the expense of time dependent simulations in large scale power and distribution systems. In both of these applications it is presumed that there is a strong influence on weather/climate, as it is this dependency that influences the reduced representation. Trigonometric polynomials are chosen here because of their spectral accuracy. Furthermore, the choice was motivated by the empirical observation that strong correlations between weather and climate and networks that are sensitive to these environmental factors will be borne out in the spectra of the weather and the network signals. In this sense, the surrogate will be endowed with interpretability. For an alternative Fourier-based approach, see (Willcox and Megretski 2005).

A lower dimensional and computationally nimble surrogate model can be a useful alternative to a very large and computationally demanding time dependent distribution model when a quick estimate of some dynamic quantity suffices. A major obstable to using Fourier methods in power distribution networks was addressed in this paper, namely, the stable (de) convolution operation, critical to quantities that appear as time dependent products/quotients. We argue that for simulations of weather-sensitive power distribution networks, a surrogate that comes equipped with the inherent variability of weather itself can prove useful in understanding the dynamics of the distribution systems. The construction of the surrogate proposed here relies on using a subset of Fourier interpolants or degrees of freedom. The subset of degrees of freedom is not chosen by a low-pass filtering or by an energetic ranking, but instead is informed by the degrees of freedom in the weather signal. In the examples presented in this paper the classification of the electrical signals was made in terms of time scales, a diurnal and a seasonal set, based upon the conjecture that both of these would be strongly identified in the consumption of power. Other classifications may be possible with this data set. Two slightly different algorithms are proposed. Both include hourly as well as diurnal scales of resolution. One of the methods picks the most salient frequencies in each time scale, the other thresholds the longer time scales and chooses salient frequencies in the fast scales. Once the Fourier interpolants are chosen, the final surrogate is constructed by tuning the amplitudes to either a data set or by constraining the amplitudes, using least squares. A possible extension of this work would pursue an optimization on both the frequency content as well as on the amplitudes of each of the modes. This would entail pinning down twice the number of degrees of freedom in the surrogate. For a distribution system that is very highly affected by weather, this approach might complicate things and yield incremental improvements. However, for a network where internal as well as external forces play a role, this approach might prove fruitful. Another follow up on this work would be to extend the strategy to a Fourier Feature Network (Kovatchi, Lanthaler, and Mishra 2021) surrogate. The goal there would be to endow the Fourier network with a prior data classification, thus curbing the training demands on the network. It is not clear, at the outset, that doing so would lead to a computationally more efficient Fourier Feature Network, as compared to the empirical spectral technique we proposed here.

ACKNOWLEDGEMENTS

This manuscript has been authored by UT-Battelle, LLC under Contract No. DE-AC05-00OR22725 with the U.S. Department of Energy. The United States Government retains and the publisher, by accepting the article for publication, acknowledges that the United States Government retains a non-exclusive, paid-up, irrevocable, worldwide license to publish or reproduce the published form of this manuscript, or allow others to do so, for United States Government purposes. The Department of Energy will provide public access to these results of federally sponsored research in accordance with the DOE Public Access Plan (http://energy.gov/downloads/doe-public-access-plan).

REFERENCES

Al-Alawi, S. and S. Islam. 1996. "Principles of electricity demand forecasting. I. Methodologies". *Power Engineering Journal* 10(3):139–143 https://doi.org/10.1049/pe:19960306.

Almeshaiei, E. and H. Soltan. 2011. "A methodology for Electric Power Load Forecasting". *Alexandria Engineering Journal* 50(2):137–144 https://doi.org/https://doi.org/10.1016/j.aej.2011.01.015.

Hu, Z., J. Ma, L. Yang, L. Yao and M. Pang. 2019. "Monthly electricity demand forecasting using empirical mode decomposition-based state space model". *Energy & Environment* 30(7):1236–1254 https://doi.org/10.1177/0958305X19842061.

Jiang, P., Q. Zhou, and X. Shao. *Surrogate Model-Based Engineering Design and Optimization*. Springer.

Kovatchi, N., S. Lanthaler, and S. Mishra. 2021. "On Universal Approximation and Error Bounds for Fourier Neural Operators". *Journal of Machine Learning Research* 22:1–76.

Olama, M., J. Dong, I. Sharma, Y. Xue and T. Kuruganti. 2020. "Frequency Analysis of Solar PV Power to Enable Optimal Building Load Control". *Energies* 13(18) https://doi.org/10.3390/en13184593.

Rastogi, D., F. Lehner, T. Kuruganti, K. J. Evans, K. Kurte and J. Sanyal. 2021, oct. "The role of humidity in determining future electricity demand in the southeastern United States". *Environmental Research Letters* 16(11):114017 https://doi.org/10.1088/1748-9326/ac2fdf.

Willcox, K. and A. Megretski. 2005. "Fourier Series for Accurate, Stable, Reduced-Order Models in Large-Scale Linear Applications". *SIAM Journal on Scientific Computing* 26(3):944–962 https://doi.org/10.1137/S1064827502418768.

AUTHOR BIOGRAPHIES

JUAN M. RESTREPO is Section Head for the Mathematics in Computing Section at Oak Ridge National Laboratory (ORNL). His research is focused on probabilistic dynamics, and the assimilation of observations and physics and machine learning models in dynamics. He is a Fellow of the Society of Industrial and Applied Mathematics, and Fellow of the American Physical Society. His email address is restrepojm@ornl.gov.

JAMES NUTARO is a Distinguished Research & Development staff member in the Computational Sciences & Engineering directorate at Oak Ridge National Laboratory. His research interests include model methods, discrete event and hybrid dynamic systems, simulation algorithms, and systems & software engineering. He serves as an associated editor for the ACM Transactions on Modeling and Computer Simulator and the journal SIMULATION. His email address is nutarojj@ornl.gov

CHRIS STICHT is a R&D and consulting engineer. His work focuses on electric power systems and machine learning. Mr. Sticht invented ATILDA, a technique for load characterization, weather adjustment and load growth algorithms. His email address is csticht@root3company.com.

TEJA KURUGANTI is Section Head for the Advanced Computing Methods for Engineered Systems at ORNL. His research interests include wireless sensor networks, modeling and simulation of communication and control systems, and electric grid modeling. His email address is kurugantipv@ornl.gov.